Journal of Sound and Vibration (1999) **219**(1), 23–33
Article No. jsvi.1998.1822, available online at http://www.idealibrary.com.on IDEAL

NATURAL FREQUENCIES OF NON-CIRCULAR ARCHES WITH ROTATORY INERTIA AND SHEAR DEFORMATION

S. J. Oh

Engineering Research Institute, *Wonkwang University*, *Iksan*, *Junbuk* 570-749, *Korea*

B. K. Lee

Department of Civil Engineering, *Wonkwang University*, *Iksan*, *Junbuk* 570-749, *Korea*

AND

I. W. Lee

Department of Civil Engineering,
Korea Advanced Institute of Science and Technology, *Taejon* 305-701, *Korea*

(*Received* 24 *February* 1998, *and in final form* 28 *May* 1998)

The differential equations governing free, in-plane vibrations of non-circular arches, including the effects of rotatory inertia, shear deformation and axial deformation, are derived and solved numerically to obtain frequencies and mode shapes. The lowest four natural frequencies are calculated for the parabolic, elliptic and sinusoidal geometries with hinged–hinged, hinged–clamped, and clamped–clamped end constraints. A wide range of arch rise to span length ratios, slenderness ratios, and two different values of shear parameter are considered. The agreement with results determined by means of a finite element method is good from an engineering viewpoint.

1. INTRODUCTION

The problem of the free vibration of arches has become a subject of interest for many investigators due to its importance in many practical applications. The governing equations and the significant historical literature on the in-plane vibrations of elastic arches are reported in references and their citations. Den Hartog [1], Wolf [2], Veletsos *et al*. [3], Laura *et al*. [4], Maurizi *et al*. [5] and Chidamparam and Leissa [6] calculated the natural frequencies of circular arches. For non-circular arches, Volterra and Morell [7], Romanelli and Laura [8], Wang [9], Gutierrez *et al*. [10], Lee and Wilson [11] and Oh [12] analyzed the free vibration of arches with various geometries. Although there is considerable research on the free vibration analysis of arches, most work has been done within the scope of Bernoulli–Euler or Rayleigh beam theory. These theories are

0022–460X/99/0100023 + 11 $30.00/0

recognized as adequate for the usual engineering problems. However, for arches having large cross-sectional dimensions in comparison with their span length, and for arches in which higher modes are required, Timoshenko beam theory which takes into account the rotatory inertia and shear effects gives a better approximation to the true behavior.

Considerable research has been devoted to study the effects of rotatory inertia and shear deformation on straight beam vibrations. In the case of arches, Austin and Veletsos [13], Davis *et al*. [14], Irie *et al*. [15, 16] and Issa *et al*. [17] included the effects of rotatory inertia and shear deformation on frequencies of circular arches. Recently, Kang *et al*. [18] computed the frequencies using the differential quadrature method; and Yildirim [19] calculated the natural frequencies using the transfer matrix method, but these are for only the circular arch, which has the simplest geometry.

For non-circular arches, Suzuki and Takahashi [20] analyzed the free vibration of elliptic arches with hinged and clamped ends; Tseng *et al*. [21] recently calculated the first six natural frequencies for parabolic and elliptic arches.

The main purpose of this paper is to investigate the free vibrations of non-circular arches based on the Timoshenko beam theory. The differential equations are derived for the in-plane free vibration of linearly elastic arches of uniform stiffness and constant mass per unit length. The effects of rotatory inertia, shear deformation and axial deformation are included.

The governing equations were solved numerically for the parabolic, elliptic and sinusoidal geometries with hinged–hinged, hinged–clamped, and clamped–clamped end constraints. The lowest four natural frequencies are calculated over a range of non-dimensional system parameters: the arch rise to span length ratio, the slenderness ratio and the shear parameter.

2. MATHEMATICAL MODEL

The geometry of the non-circular arch with uniform cross-section, symmetric about the crown, is defined in Figure 1(a). Its span length, rise, and shape of the middle surface are l, h, and $y(x)$, respectively. Its radius of curvature ρ, a function

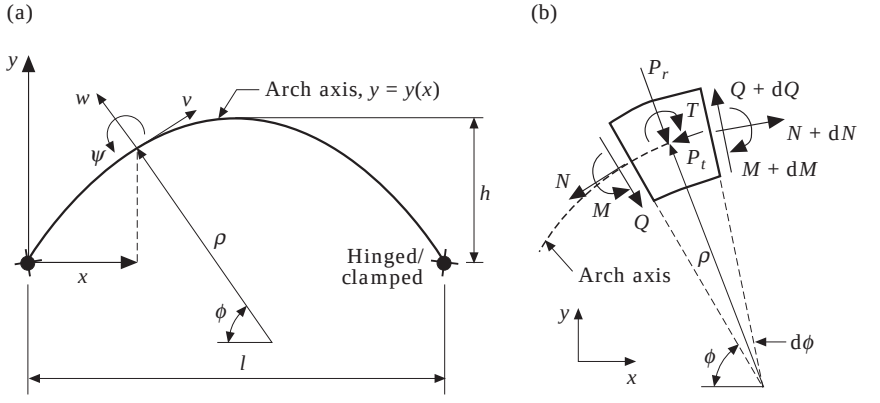

Figure 1. (a) Arch geometry; (b) loads on an arch element.

of the co-ordinate x, has an inclination ϕ with the x-axis. Shown in Figure 1(a) are the positive directions of radial and tangential displacements, w and v, and positive direction of the rotation angle ψ of the cross section at point ϕ.

A small element of the arch shown in Figure 1(b) defines the positive directions for its loads: the axial forces N; the shear forces Q; the bending moments M; the radial inertia force P_r; the tangential inertia force P_t; and rotatory inertia couple T. With the inertia forces and the inertia couple treated as equivalent static quantities, the three equations for "dynamic equilibrium" of the element are

$$\mathrm{d}N/\mathrm{d}\phi + Q - \rho P_t = 0, \qquad \mathrm{d}Q/\mathrm{d}\phi - N - \rho P_r = 0,$$
$$(1/\rho)\,\mathrm{d}M/\mathrm{d}\phi - Q + T = 0. \tag{1–3}$$

The rotation of the tangent to the centroidal axis, given in reference [22], is

$$\Phi = (1/\rho)(\mathrm{d}w/\mathrm{d}\phi - v). \tag{4}$$

When shear deformation is considered, the rotation of the tangent to the centroidal axis may be expressed as

$$\Phi = \psi + \beta, \tag{5}$$

where β is the angular deformation due to shear.

From equations (4) and (5), one obtains

$$\beta = (1/\rho)(\mathrm{d}w/\mathrm{d}\phi - v - \rho\psi). \tag{6}$$

The bending moment, normal force and shear force with inclusion of the effects of rotatory inertia, shear deformation and axial deformation, as given in reference [23] are

$$M = -(EI/\rho)\psi', \qquad N = (EA/\rho)(v' + w) + (EI/\rho^2)\psi',$$
$$Q = kAG\beta = (kAG/\rho)(w' - v - \rho\psi), \tag{7–9}$$

where $(') = \mathrm{d}/\mathrm{d}\phi$, E is the Young's modulus, I is the area moment of inertia of cross-section, A is the cross-sectional area, k is the shape factor of cross-section, and G is the shear modulus.

The arch is assumed to be in harmonic motion, or each displacement component is proportional to $\sin(\omega t)$, where ω is the angular frequency and t is time. The inertia loadings are then

$$P_r = -\gamma A\omega^2 w, \qquad P_t = -\gamma A\omega^2 v, \qquad T = -\gamma I\omega^2\psi, \tag{10–12}$$

where γ is mass density of arch material.

To facilitate the numerical studies, the following non-dimensional system variables are defined. The arch rise to span length ratio f, the slenderness ratio s and the shear parameter μ are, respectively,

$$f = h/l, \qquad s = l/\sqrt{I/A}, \qquad \mu = kG/E. \tag{13–15}$$

The co-ordinates, the displacements and the radius of curvature are normalized by the span length l:

$$\xi = x/l, \quad \eta = y/l; \qquad \delta = w/l, \quad \lambda = v/l; \qquad \zeta = \rho/l. \tag{16–18}$$

The frequency parameter is

$$C_i = \omega_i s l \sqrt{\gamma/E}, \tag{19}$$

which is written in terms of the ith frequency $\omega = \omega_i$, $i = 1, 2, 3, 4, \ldots$.

When equations (7–12) are substituted into equations (1–3) and the non-dimensional forms of equations (13–19) are used, the results are

$$\delta'' = \zeta^{-1}\zeta'\delta' + \mu^{-1}(1 - \zeta^2 s^{-2} C_i^2)\delta + (1 + \mu^{-1})\lambda' - \zeta^{-1}\zeta'\lambda + (\zeta + \mu^{-1}\zeta^{-1}s^{-2})\psi', \tag{20}$$

$$\lambda'' = \zeta^{-1}\zeta'\lambda' + (\mu - \zeta^2 s^{-2} C_i^2)\lambda - (1 + \mu)\delta' + \zeta^{-1}\zeta'\delta - \zeta^{-1}s^{-2}\psi'' + 2\zeta^{-2}\zeta' s^{-2}\psi' + \mu\zeta\psi, \tag{21}$$

$$\psi'' = \zeta^{-1}\zeta'\psi' + (\mu s^2 - s^{-2} C_i^2)\zeta^2\psi - \zeta\mu s^2\delta' + \zeta\mu s^2\lambda. \tag{22}$$

The boundary conditions for hinged ends are

$$\delta = 0, \qquad \lambda = 0, \qquad \psi' = 0, \tag{23}$$

where the last condition assures that the moment M given by equation (7) is zero.

The boundary conditions for clamped ends are

$$\delta = 0, \qquad \lambda = 0, \qquad \psi = 0. \tag{24}$$

3. GEOMETRIC FUNCTIONS: ϕ, ζ AND ζ'

The geometric functions ϕ, ζ and ζ' contained in the governing differential equations (20–22) are computed as follows [11]. The non-dimensional form of the given arch shape $y = y(x)$ is

$$\eta = \eta(\xi). \tag{25}$$

By definition

$$\phi = \pi/2 - \tan^{-1}(\mathrm{d}\eta/\mathrm{d}\xi), \qquad \zeta = (\mathrm{d}^2\eta/\mathrm{d}\xi^2)^{-1}[1 + (\mathrm{d}\eta/\mathrm{d}\xi)^2]^{3/2}. \tag{26, 27}$$

Both ϕ and ζ are computed from derivatives of equation (25) and are expressed as functions of the single variable χ. Then ξ' is calculated from the derivatives of equations (26) and (27) by using

$$\zeta' = (\mathrm{d}\zeta/\mathrm{d}\xi)(\mathrm{d}\xi/\mathrm{d}\phi). \tag{28}$$

The non-dimensional equation for the parabolic arch of span length l and rise h is

$$\eta = -4f\xi(\xi - 1), \qquad 0 \leqslant \xi \leqslant 1. \tag{29}$$

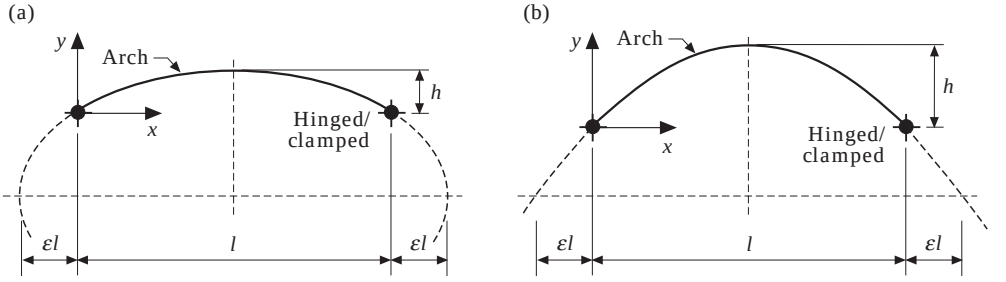

Figure 2. Arch shapes: (a) elliptic; (b) sinusoidal.

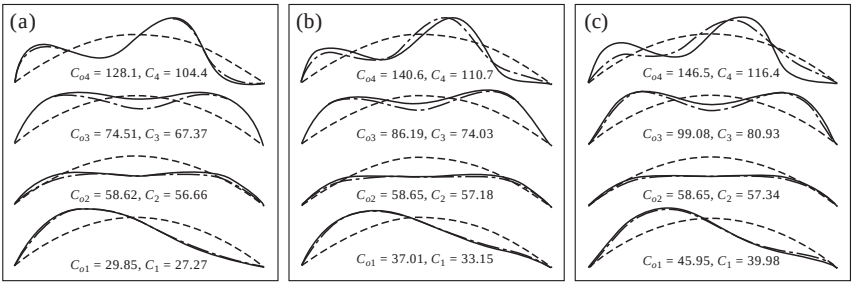

Figure 3. Examples of mode shapes. (a) Hinged–hinged; (b) hinged–clamped; (c) clamped–clamped.

The general equation for the elliptic arch in non-dimensional form, which has span length l, rise h, and a co-ordinate system (x, y) originating from the left support as shown in Figure 2(a), is

$$\eta = (b_2/b_1)[b_1^2 - (\xi - 1/2)^2]^{1/2} + f - b_2, \quad 0 \leqslant \xi \leqslant 1, \tag{30a}$$

TABLE 1

Comparison of results between finite element method (ADINA) and this study

Geometry of arch	i	Frequency parameter, C_i	
		ADINA	This study
Parabolic	1	21·81	21·83
hinged–hinged,	2	55·80	56·00
$f = 0{\cdot}3$, $s = 75$,	3	101·7	102·3
$\mu = 0{\cdot}3$	4	113·4	113·4
Elliptic ($\epsilon = 0{\cdot}5$)	1	35·26	35·25
hinged–clamped,	2	56·99	57·11
$f = 0{\cdot}2$, $s = 50$,	3	83·05	83·00
$\mu = 0{\cdot}3$	4	128·1	128·2
Sinusoidal ($\epsilon = 0{\cdot}5$)	1	56·25	56·30
clamped–clamped,	2	66·25	66·14
$f = 0{\cdot}1$, $s = 100$,	3	114·9	114·3
$\mu = 0{\cdot}3$	4	181·7	181·7

TABLE 2

Frequency parameter C_i for hinged–hinged arches

			Frequency parameter C_i							
			$\mu = 0{\cdot}1$				$\mu = 0{\cdot}3$			
f	s	Shape†	$i = 1$	$i = 2$	$i = 3$	$i = 4$	$i = 1$	$i = 2$	$i = 3$	$i = 4$
0·01	30	Parabolic	9·650	33·23	63·77	94·16	9·974	37·47	79·21	94·25
		Elliptic	9·654	33·23	63·77	94·10	9·979	37·46	79·21	94·25
		Sinusoidal	9·646	33·24	63·77	94·19	9·971	37·47	79·21	94·25
	60	Parabolic	10·66	37·61	80·15	133·0	10·74	38·94	86·25	149·9
		Elliptic	10·68	37·61	80·16	133·0	10·76	38·94	86·26	149·9
		Sinusoidal	10·65	37·61	80·15	133·0	10·73	38·94	86·25	149·9
	100	Parabolic	12·17	38·76	85·43	147·5	12·20	39·26	87·88	154·9
		Elliptic	12·22	38·76	85·45	147·5	12·25	39·26	87·91	154·9
		Sinusoidal	12·15	38·76	85·41	147·5	12·17	39·26	87·87	154·9
0·1	30	Parabolic	22·31	30·54	60·93	89·71	22·48	34·21	74·94	93·87
		Elliptic	22·39	30·40	61·08	88·57	22·59	34·05	75·00	93·82
		Sinusoidal	22·23	30·64	60·86	90·52	22·38	34·32	74·93	93·84
	60	Parabolic	34·48	41·53	76·92	126·0	35·64	41·67	82·26	141·1
		Elliptic	34·33	41·32	77·80	125·3	35·47	41·56	83·02	140·2
		Sinusoidal	34·59	41·57	76·44	126·4	35·75	41·66	81·86	141·6
	100	Parabolic	35·51	64·24	86·66	139·4	35·95	64·76	88·35	146·0
		Elliptic	35·35	62·03	90·24	138·8	35·79	62·69	91·79	145·3
		Sinusoidal	35·62	65·72	84·31	139·7	36·06	66·10	86·14	146·4
0·2	30	Parabolic	24·80	36·50	53·72	81·56	27·40	36·79	64·52	91·23
		Elliptic	24·49	36·21	54·29	80·29	27·04	36·75	64·73	91·01
		Sinusoidal	25·03	36·59	53·48	82·36	27·66	36·74	64·48	91·18
	60	Parabolic	27·76	61·71	76·63	110·4	28·57	64·64	77·88	122·2
		Elliptic	27·40	59·26	79·90	109·3	28·20	61·99	81·33	120·8
		Sinusoidal	28·02	63·45	74·40	111·0	28·84	66·64	75·41	122·9
	100	Parabolic	28·52	67·10	120·8	123·1	28·83	68·68	123·3	125·9
		Elliptic	28·15	65·24	119·8	126·4	28·46	66·74	124·7	126·8
		Sinusoidal	28·79	68·18	121·2	121·5	29·10	69·80	121·3	126·6
0·3	30	Parabolic	19·20	43·35	46·60	71·09	20·89	45·42	52·51	85·65
		Elliptic	18·84	41·89	48·18	70·34	20·48	44·81	53·16	85·09
		Sinusoidal	19·48	44·33	45·56	71·47	21·20	45·50	52·43	85·43
	60	Parabolic	21·21	52·72	90·90	92·53	21·73	55·52	91·03	101·0
		Elliptic	20·80	51·85	91·70	92·20	21·30	54·57	92·43	99·99
		Sinusoidal	21·52	53·12	90·29	93·00	22·04	55·97	90·37	101·5
	100	Parabolic	21·72	55·27	99·93	146·1	21·90	56·37	103·4	148·5
		Elliptic	21·29	54·46	99·04	145·7	21·47	55·54	102·5	148·9
		Sinusoidal	22·03	55·66	100·4	146·4	22·21	56·77	104·0	148·2
0·4	30	Parabolic	14·78	36·11	49·20	60·04	15·86	41·58	49·28	73·95
		Elliptic	14·44	35·85	49·46	59·73	15·48	41·22	49·58	73·85
		Sinusoidal	15·04	36·14	49·21	60·13	16·14	41·56	49·38	73·46
	60	Parabolic	16·11	42·10	75·66	97·29	16·42	43·96	81·37	97·77
		Elliptic	15·72	41·79	75·15	97·62	16·03	43·61	80·79	98·19
		Sinusoidal	16·40	42·21	75·94	97·23	16·71	44·08	81·69	97·68
	100	Parabolic	16·43	43·77	80·71	124·8	16·52	44·49	83·02	130·1
		Elliptic	16·04	43·44	80·13	123·9	16·13	44·14	82·41	129·2
		Sinusoidal	16·72	43·91	81·05	125·3	16·81	44·63	83·38	130·7

† For the elliptic and sinusoidal arches, $\epsilon = 0{\cdot}5$.

TABLE 3

Frequency parameter C_i for hinged–clamped arches

			Frequency parameter C_i							
			$\mu = 0{\cdot}1$				$\mu = 0{\cdot}3$			
f	s	Shape†	$i = 1$	$i = 2$	$i = 3$	$i = 4$	$i = 1$	$i = 2$	$i = 3$	$i = 4$
0·01	30	Parabolic	13·71	37·67	66·99	94·20	14·91	45·11	87·30	94·25
		Elliptic	13·71	37·67	66·99	94·16	14·91	45·11	87·30	94·25
		Sinusoidal	13·71	37·67	66·99	94·22	14·91	45·11	87·30	94·25
	60	Parabolic	15·44	45·81	89·55	142·1	15·79	48·61	99·29	165·2
		Elliptic	15·45	45·81	89·56	142·0	15·80	48·61	99·29	165·1
		Sinusoidal	15·44	45·81	89·54	142·1	15·79	48·62	99·28	165·2
	100	Parabolic	16·70	48·33	98·20	162·3	16·82	49·45	102·4	173·3
		Elliptic	16·71	48·33	98·20	162·3	16·83	49·44	102·4	173·2
		Sinusoidal	16·69	48·33	98·19	162·3	16·81	49·45	102·4	173·3
0·1	30	Parabolic	23·53	35·05	64·30	90·59	24·08	41·61	82·93	93·88
		Elliptic	23·53	34·90	64·47	89·46	24·10	41·44	83·00	93·82
		Sinusoidal	23·51	35·16	64·21	91·39	24·06	41·75	82·89	93·88
	60	Parabolic	39·62	44·22	86·26	134·6	40·48	46·00	94·87	155·1
		Elliptic	39·75	43·60	86·98	133·8	40·60	45·46	95·43	153·9
		Sinusoidal	39·48	44·66	85·83	135·1	40·34	46·40	94·54	155·8
	100	Parabolic	44·12	64·54	97·86	153·6	45·09	65·00	101·1	163·4
		Elliptic	44·15	62·70	100·3	152·9	45·13	63·31	103·4	162·6
		Sinusoidal	44·08	65·79	96·28	154·0	45·04	66·14	99·70	163·8
0·2	30	Parabolic	28·33	37·10	57·42	83·17	32·37	38·31	72·17	91·23
		Elliptic	28·11	36·59	58·00	81·74	32·25	37·87	72·39	91·05
		Sinusoidal	28·49	37·39	57·11	84·14	32·44	38·61	72·07	91·22
	60	Parabolic	34·23	64·76	81·63	118·6	35·97	67·20	85·93	134·8
		Elliptic	33·98	62·13	84·54	117·4	35·73	64·82	88·51	133·2
		Sinusoidal	34·40	66·75	79·50	119·4	36·14	68·91	84·15	135·8
	100	Parabolic	35·98	75·98	122·9	134·2	36·68	78·54	123·5	141·5
		Elliptic	35·72	73·44	125·3	133·7	36·42	75·87	126·5	140·4
		Sinusoidal	36·16	77·62	121·2	134·7	36·86	80·29	121·6	142·1
0·3	30	Parabolic	22·60	44·00	49·69	73·39	25·75	45·49	59·57	85·65
		Elliptic	22·29	42·58	51·08	72·46	25·41	44·83	60·06	85·40
		Sinusoidal	22·84	44·98	48·75	73·90	25·99	45·83	59·38	85·56
	60	Parabolic	26·56	59·54	90·99	100·5	27·68	64·03	91·41	112·3
		Elliptic	26·20	58·20	92·15	99·76	27·32	62·47	92·90	111·2
		Sinusoidal	26·81	60·30	90·38	101·0	27·95	64·93	90·64	113·0
	100	Parabolic	27·69	64·03	110·9	147·7	28·13	65·93	116·2	149·1
		Elliptic	27·33	62·85	109·8	148·0	27·76	64·71	115·0	149·9
		Sinusoidal	27·96	64·70	111·6	147·7	28·39	66·63	116·9	148·7
0·4	30	Parabolic	17·77	39·41	49·43	62·72	19·86	47·00	49·97	78·28
		Elliptic	17·47	38·85	49·86	62·33	19·52	45·73	51·02	78·11
		Sinusoidal	18·00	39·63	49·32	62·87	20·11	47·66	49·48	77·53
	60	Parabolic	20·39	48·53	82·81	97·31	21·09	51·63	91·07	97·77
		Elliptic	20·05	47·99	82·15	97·63	20·74	51·04	90·25	98·22
		Sinusoidal	20·65	48·79	83·19	97·28	21·36	51·93	91·53	97·68
	100	Parabolic	21·11	51·41	90·26	134·6	21·36	52·66	93·77	141·6
		Elliptic	20·75	50·86	89·53	133·6	21·01	52·09	93·00	140·4
		Sinusoidal	21·37	51·69	90·69	135·3	21·62	52·95	94·24	142·3

† For the elliptic and sinusoidal arches, $\epsilon = 0{\cdot}5$.

TABLE 4

Frequency parameter C_i for clamped–clamped arches

			Frequency parameter C_i							
			$\mu = 0{\cdot}1$				$\mu = 0{\cdot}3$			
f	s	Shape†	$i = 1$	$i = 2$	$i = 3$	$i = 4$	$i = 1$	$i = 2$	$i = 3$	$i = 4$
0·01	30	Parabolic	18·10	41·68	69·96	94·21	20·75	52·72	94·25	95·00
		Elliptic	18·10	41·68	69·96	94·19	20·75	52·72	94·25	95·00
		Sinusoidal	18·10	41·68	69·96	94·22	20·75	52·72	94·25	95·00
	60	Parabolic	21·37	54·18	98·70	150·7	22·26	59·05	112·7	180·4
		Elliptic	21·37	54·18	98·70	150·7	22·25	59·04	112·7	180·3
		Sinusoidal	21·38	54·18	98·69	150·7	22·27	59·05	112·7	180·4
	100	Parabolic	22·83	58·62	111·3	177·2	23·17	60·66	117·8	192·3
		Elliptic	22·81	58·62	111·4	177·2	23·15	60·66	117·8	192·3
		Sinusoidal	22·85	58·63	111·3	177·2	23·18	60·67	117·8	192·3
0·1	30	Parabolic	25·93	38·85	67·42	91·14	27·43	48·71	90·62	93·88
		Elliptic	25·80	38·73	67·60	90·06	27·29	48·57	90·67	93·82
		Sinusoidal	26·01	38·94	67·31	91·88	27·52	48·82	90·60	93·88
	60	Parabolic	42·89	50·36	95·36	142·7	43·26	54·69	107·9	168·0
		Elliptic	42·28	50·23	95·98	141·7	42·71	54·56	108·3	166·3
		Sinusoidal	43·29	50·45	94·97	143·3	43·63	54·79	107·6	169·2
	100	Parabolic	54·39	64·61	110·1	167·6	56·21	65·04	115·4	181·2
		Elliptic	54·26	62·85	111·9	166·8	56·08	63·43	117·0	180·4
		Sinusoidal	54·49	65·81	108·9	168·1	56·30	66·14	114·3	181·7
0·2	30	Parabolic	32·71	37·27	60·83	84·41	38·11	40·17	79·68	91·23
		Elliptic	32·42	36·69	61·41	82·87	37·71	39·85	79·87	91·06
		Sinusoidal	32·91	37·62	60·50	85·51	38·37	40·42	79·60	91·23
	60	Parabolic	41·78	66·01	88·59	126·2	44·96	67·95	96·53	146·9
		Elliptic	41·45	63·52	91·03	124·7	44·62	65·89	98·40	144·8
		Sinusoidal	42·01	67·82	86·86	127·2	45·21	69·37	95·30	148·3
	100	Parabolic	44·84	84·10	125·6	146·2	46·16	87·63	126·5	156·7
		Elliptic	44·51	80·76	128·8	144·8	45·82	84·07	129·9	155·1
		Sinusoidal	45·09	86·45	123·4	147·1	46·41	90·17	124·2	157·7
0·3	30	Parabolic	26·43	44·15	53·00	75·37	31·66	45·50	66·60	85·65
		Elliptic	26·09	42·85	54·19	74·24	31·26	44·83	66·97	85·48
		Sinusoidal	26·68	45·03	52·24	76·04	31·95	45·91	66·44	85·59
	60	Parabolic	32·91	65·93	92·09	107·8	35·01	72·10	93·06	123·5
		Elliptic	32·50	63·99	93·75	106·6	34·58	69·72	95·08	121·9
		Sinusoidal	33·21	67·15	91·13	108·5	35·33	73·68	91·79	124·5
	100	Parabolic	34·99	73·11	122·3	148·2	35·83	76·06	129·7	149·2
		Elliptic	34·56	71·47	121·1	148·6	35·40	74·34	128·3	150·1
		Sinusoidal	35·30	74·08	123·1	148·0	36·15	77·10	130·6	148·8
0·4	30	Parabolic	21·18	42·26	49·92	65·15	24·72	48·63	54·58	78·35
		Elliptic	20·85	41·33	50·66	64·63	24·34	47·49	55·40	78·38
		Sinusoidal	21·42	42·76	49·59	65·37	25·00	49·30	54·17	78·03
	60	Parabolic	25·63	55·05	89·87	97·32	26·96	59·78	97·77	101·1
		Elliptic	25·23	54·26	89·13	97·63	26·54	58·87	98·22	100·2
		Sinusoidal	25·92	55·47	90·30	97·29	27·27	60·27	97·68	101·6
	100	Parabolic	26·97	59·52	100·1	143·4	27·48	61·51	105·1	150·9
		Elliptic	26·55	58·75	99·21	142·1	27·06	60·71	104·1	149·7
		Sinusoidal	27·28	59·94	100·6	144·2	27·79	61·96	105·6	151·8

† For the elliptic and sinusoidal arches, $\epsilon = 0{\cdot}5$.

where

$$b_1 = (1 + 2\epsilon)/2, \qquad b_2 = f/[1 - 2(\epsilon + \epsilon^2)^{1/2}/(1 + 2\epsilon)]. \tag{30b, c}$$

Finally, the non-dimensional equation for the sinusoidal arch shown in Figure 2(b) is

$$\eta = f - c_1 + c_1 \sin(c_2\xi + c_2\epsilon), \qquad 0 \leqslant \xi \leqslant 1, \tag{31a}$$

where

$$c_1 = f/[1 - \sin(c_2\epsilon)], \qquad c_2 = \pi/(1 + 2\epsilon). \tag{31b, c}$$

For the above arch geometries, ϕ, ζ and ζ' are calculated in a straightforward manner from equations (29–31), respectively, with use of equations (26–28).

4. NUMERICAL METHOD AND COMPUTED RESULTS

Based on the above analysis, a general Fortran computer program was written to calculate the frequency parameters C_i and the corresponding mode shapes $\delta = \delta_i(\xi)$ and $\lambda = \lambda_i(\xi)$. The numerical methods similar to those described by Veletsos *et al*. [3] and Lee and Wilson [11] were used to solve the differential equations (20–22), subject to the end constraints as given in equations (23) and (24). The hinged–hinged, hinged–clamped and clamped–clamped end constraints were considered for each of the three arch geometries, for given parameters f, s, μ and ϵ. (Recall that ϵ is needed for elliptic and sinusoidal geometries only.) First, the Determinant Search Method combined with the Regula–Falsi method was used to calculate the characteristic values C_i, and then the Runge–Kutta method was used to calculate the mode shapes. In this study, the lowest four values of C_i and the corresponding mode shapes were calculated.

The numerical results are shown in Tables 1–4 and Figure 3. A value of $\mu = 0{\cdot}1$ corresponds to a wide-flange steel section and $\mu = 0{\cdot}3$ corresponds approximately to a solid rectangular metal section.

The first series of numerical studies are shown in Table 1. These studies served as an approximate check on the analysis presented herein. For comparison purposes, finite element solutions based on the finite element program ADINA were used to compute the lowest four frequency parameters C_i for three cases: a hinged–hinged parabolic arch with $f = 0{\cdot}3$, $s = 75$ and $\mu = 0{\cdot}3$; a hinged–clamped elliptic arch with $f = 0{\cdot}2$, $s = 50$, $\mu = 0{\cdot}3$ and $\epsilon = 0{\cdot}5$; and a clamped–clamped sinusoidal arch with $f = 0{\cdot}1$, $s = 100$, $\mu = 0{\cdot}3$ and $\epsilon = 0{\cdot}5$. The ADINA results were calculated using 100 beam elements. The agreement is good for all cases considered.

Tables 2–4 depict the lowest four values of the frequency parameters C_i for parabolic, elliptic and sinusoidal geometries with hinged–hinged, hinged–clamped and clamped–clamped end constraints. From these and other results, the following conclusions were reached. (1) The C_i values always increase as the slenderness ratio s increases. (2) The C_i values are always somewhat higher with $\mu = 0{\cdot}3$ than with $\mu = 0{\cdot}1$, other parameters remaining constant. (3) For a given set of arch parameters and matching end constraints, the arch geometry has little effect on

the frequency parameters C_i. (4) As the end constraint increases on all three arch geometries, from hinged–hinged to hinged–clamped to clamped–clamped, each value of C_i increases, other parameters remaining constant.

Shown in Figure 3 are the computed frequency parameters C_i and their corresponding mode shapes for hinged–hinged, hinged–clamped and clamped–clamped parabolic arches with $f = 0{\cdot}2$, $s = 50$ and $\mu = 0{\cdot}1$. In Figure 3, the C_{oi} values and the chain line are the frequency parameters and their corresponding mode shapes for arch without rotatory inertia and shear deformation as obtained by Oh [12].

5. CONCLUSIONS

The differential equations for in-plane vibrations of noncircular arches, including the effects of rotatory inertia, shear deformation and axial deformation, were derived and solved numerically. There is very good agreement between the results of the present analysis and ADINA. For three arch geometries (parabolic, elliptic and sinusoidal), the effects of each of the three parameters f, s and μ on C_i were investigated. The methods presented here for calculating frequencies and mode shapes for noncircular arches were found to be efficient and reliable over a wide range of system parameters. In this paper, numerical results were provided only for the parabolic, elliptic and sinusoidal arches; however, the approach presented here can also be extended to arches of other geometries with little effort in section 3.

ACKNOWLEDGMENTS

The first author extends his thanks to the Korea Science and Engineering Foundation for financial support; and to Korea Advanced Institute of Science and Technology for providing the facilities and the appointment of Post-Doctoral Fellow to do this research in 1997.

REFERENCES

1. J. P. Den Hardog 1928 *Philosophical Magazine* **5,** 400–408. The lowest natural frequency of circular arcs.
2. J. A. Wolf Jr. 1971 *Journal of the Structural Division*, *American Society of Civil Engineers* **97,** 2337–2350. Natural frequencies of circular arches.
3. A. S. Veletsos, W. J. Austin, C. A. L. Pereira and S. J. Wung 1972 *Journal of the Engineering Mechanic Division*, *American Society of Civil Engineers* **98,** 311–329. Natural frequencies of circular arches.
4. P. A. A. Laura, P. L. Verniere De Irassar, R. Carnicer and R. Bertero 1988 *Journal of Sound and Vibration* **120,** 95–105. A note on vibrations of a circumferential arch with thickness varying in a discontinuous fashion.
5. M. J. Maurizi, R. E. Rossi and P. M. Belles 1991 *Journal of Sound and Vibration* **144,** 357–361. Lowest natural frequency of clamped circular arcs of linearly tapered width.
6. P. Chidamparam and A. W. Leissa 1995 *Journal of Sound and Vibration* **183,** 779–795. Influence of centerline extensibility on the in-plane free vibrations of loaded circular arches.

7. E. Volterra and J. D. Morell 1960 *Journal of Applied Mechanics* **27,** 744–746. A note on the lowest natural frequency of elastic arcs.
8. E. Romanelli and P. A. A. Laura 1972 *Journal of Sound and Vibration* **24,** 17–22. Fundamental frequencies of non-circular, elastic, hinged arcs.
9. T. M. Wang 1975 *Journal of Sound and Vibration* **41,** 247–251. Effect of variable curvature on fundamental frequency of clamped parabolic arcs.
10. R. H. Gutierrez, P. A. A. Laura, R. E. Rossi, R. Bertero and A. Villaggi 1989 *Journal of Sound and Vibration* **129,** 181–200. In-plane vibrations of non-circular arcs of non-uniform cross-section.
11. B. K. Lee and J. F. Wilson 1989 *Journal of Sound and Vibration* **136,** 75–89. Free vibrations of arches with variable curvature.
12. S. J. Oh 1997 *Ph.D. Thesis*, *Wonkwang University*. Free vibrations of arches with variable cross-section.
13. W. J. Austin and A. S. Veletsos 1973 *Journal of the Engineering Mechanics Division*, *American Society of Civil Engineers* **99,** 735–753. Free vibration of arches flexible in shear.
14. R. Davis, R. D. Henshell and G. B. Warburton 1972 *Journal of Sound and Vibration* **25,** 561–576. Constant curvature beam finite elements for in-plane vibration.
15. T. Irie, G. Yamada and K. Takahashi 1979 *Ingenieur-Archiv* **48,** 337–346. In-plane vibration of Timoshenko arcs with variable cross-section.
16. T. Irie, G. Yamada and K. Tanaka 1983 *Journal of Applied Mechanics* **50,** 449–452. Natural frequencies of in-plane vibration of arcs.
17. M. S. Issa, T. M. Wang and B. T. Hsiao 1987 *Journal of Sound and Vibration* **114,** 297–308. Extensional vibrations of continuous circular curved beams with rotary inertia and shear deformation, I: free Vibration.
18. K. Kang, C. W. Bert and A. G. Striz 1995 *Journal of Sound and Vibration* **181,** 353–360. Vibration analysis of shear deformable circular arches by the differential quadratic method.
19. V. Yildirim 1997 *Computers & Structures* **62,** 475–485. A computer program for the free vibration analysis of elastic arcs.
20. K. Suzuki and S. Takahashi 1979 *Bulletin of the Japan Society of Mechanical Engineers* **22,** 1284–1292. In-plane vibrations of curved bars considering shear deformation and rotatory inertia.
21. Y. P. Tseng, C. S. Huang and C. J. Lin 1997 *Journal of Sound and Vibration* **207,** 15–31. Dynamic stiffness analysis for in-plane vibrations of arches with variable curvature.
22. J. Henrych 1981 *The Dynamics of Arches and Frames*. Amsterdam: Elsevier.
23. S. F. Borg and J. J. Gennaro 1959 *Advanced Structural Analysis*. New Jersey: Van Nostrand.